Quantifying Relationships among the Molecular Weight Distribution, Non-Newtonian Shear Viscosity, and Melt Index for Linear Polymers

Kevin C. Seavey, Y. A. Liu,* and Neeraj P. Khare

Honeywell Center of Excellence in Computer-Aided Design and SINOPEC/AspenTech Center of Excellence in Process Systems Engineering, Department of Chemical Engineering, Virginia Polytechnic Institute and State University, Blacksburg, Virginia 24061

Tim Bremner

Aspen Technology, Inc., 1293 Eldridge Parkway, Houston, Texas 77077

Chau-Chyun Chen

Aspen Technology, Inc., Ten Canal Park, Cambridge, Massachusetts 02141

This paper presents methodologies to quantify the relationships among the molecular weight distribution (MWD), steady-shear non-Newtonian viscosity (i.e., flow curve), and melt index (MI) of three linear low-density polyethylenes manufactured using the same technology. With the aid of computer-aided process simulation tools (such as POLYMERS PLUS), polymer producers can predict accurately the MWD from manufacturing conditions. Our methodologies help the polymer producers to extend their simulation model to predict flow curves and MI from the MWD. To do this, this paper employs (1) a modified Carreau-Yasuda (CY) model or Bersted's partition model to relate the MWDs and flow curves, (2) Bremner and Rudin's model to relate the weight-average molecular weight (MWW) and MI, and (3) Rohlfing and Janzen's model to relate the flow curve and MI. We show that the Carreau-Yasuda, Bersted, and Bremner and Rudin models work very well for correlating our data, predicting flow curves that average 3−7% error and MI values that average 2% error. In addition, for the case in which we lack MI data, we use the CY or Bersted model predictions of the flow curve to generate MI values through Rohlfing and Janzen's model. These predictions are very good, averaging only 0.5−3% error. We also show how to use the CY or Bersted model and Rohlfing and Janzen's melt-indexer model to estimate closely the low shear rate region of the flow curve using MWD/MI data alone. This case corresponds to one in which we lack flow curve data. Last, we provide practical guidelines for polymer manufacturers who want to predict the flow curve and MI using the MWD.

Introduction

Polyolefin manufacturers are interested in the rheological properties of their products. Two such properties are the steady-shear non-Newtonian viscosity, or flow curve, and the melt index (MI).[1] Knowledge of the flow curve allows for the design of polymer processing equipment,[2] while knowledge of the melt index enables more effective quality control.[3]

Current modeling tools, such as POLYMERS PLUS (Aspen Technology, Inc., Cambridge, MA), accurately simulate the production of many different polymers. Examples include low-density polyethylene (LDPE)[4] and high-density polyethylene (HDPE).[5] These software tools use thermodynamic and kinetic principles to predict accurately the production rate and entire molecular weight distribution (MWD) from reactor operating conditions and process feeds. Since polyolefin manufacturers can accurately predict the MWD, they naturally are curious about the potential to predict the flow curve and MI using the MWD.

When given the opportunity to model or otherwise predict the MI or flow curve in an industrial process in essentially real time, often the response is "Why not just measure it?". This may work well for processes with long reactor holdup times and slow process dynamics, but in many instances, the time required to sample and measure the melt properties will be longer than one or more reactor holdup times. Relying on the measurement to tell us whether we are on-spec for prime production is not an economical way to operate a polymerization facility if we can accurately predict the true MI or flow characteristics of the material in essentially real time.

More complex reaction systems (with multiple reactors and multiple catalysts, etc.) may manufacture resins that are undercharacterized by simply using the melt index as the prime grade criterion. In such cases, the ability to predict the steady-shear viscosity across a range of shear rates will aid in ensuring that the downstream resin converter is receiving material with nominally the same processing characteristics in their extrusion equipment. The ability to reproducibly predict and therefore control the flow characteristics of the resin at the reactor can only decrease the lot-to-lot variability in processing performance seen by the converter.

Three options exist for polymer manufacturers who (1) have process models that predict accurately the

* To whom correspondence should be addressed. Phone: (540) 231-7800. Fax: (540) 231-5022. E-mail: design@vt.edu.

10.1021/ie021003i CCC: $25.00
Published on Web 09/16/2003

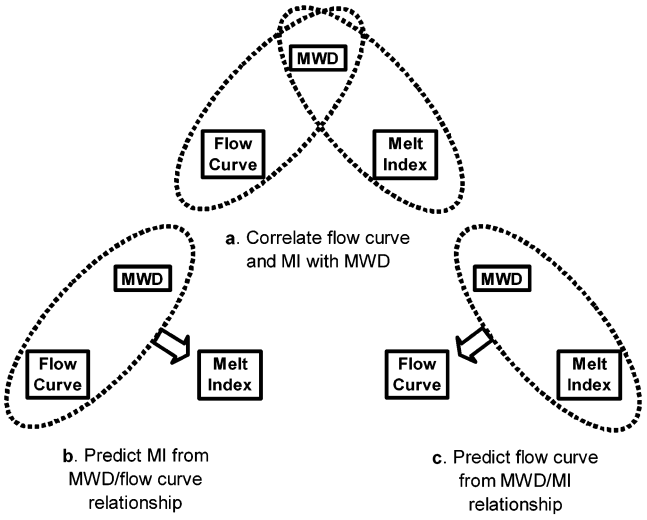

Figure 1. Three options for relating the MWD, flow curve, and MI: (a) correlate the flow curve and MI with MWD, (b) correlate the flow curve with MWD, then predict the MI, and (c) correlate the MI with MWD, then predict the flow curve.

MWD from manufacturing conditions and (2) wish to extend this model to predict flow curves and the melt index:

(a) We can correlate both the MI and flow curve with the MWD. To do this, we regress the parameters of a modified Carreau-Yasuda (CY) model or the Bersted model[6,7] using the MWD/flow curve data. Second, we use Bremner and Rudin's MWD-MI correlation[8] to compute the MI from the weight-average molecular weight. Pragmatically, we can use any general relationship between one of the molecular-weight averages and the MI, whether through log/log transform or some power-scaling law. We find that the Bremner and Rudin's correlation[8] works for the resins in this study and has a justifiable fundamental basis.

(b) We can predict the MI using the MWD/flow curve correlation. In this case, we regress the parameters of a CY or Bersted model,[6,7] as mentioned above. We then use Rohlfing and Janzen's fundamental, parameter-free melt-indexer model[9] to predict the MI using the flow curve.

(c) We can predict the flow curve using the MWD/MI correlation. We do this by regressing the flow curve parameters of the CY or Bersted[6,7] model that generate accurate MI predictions.

The purpose of this paper is to characterize these three options and to give practical guidelines for developing these relationships. Mavrides and Shroff[10] evaluated the prediction of the flow curve from the MWD using the Bersted model.[6,7] However, to our knowledge, no one has attempted to predict the MI using a CY or Bersted flow curve correlation, nor has anyone attempted to predict the flow curve using only MWD and MI data. Figure 1 illustrates the proposed options for relating the MWD, flow curve, and MI.

Correlating the Flow Curve with the MWD. We can correlate the MWD using two approaches. The first approach uses a modified CY model and requires only the weight-average molecular weight, $\overline{M_w}$. The second approach uses Bersted's partition model and requires the entire MWD.

1. Correlating the Flow Curve with the Weight-Average Molecular Weight. If we combine the Carreau-Yasuda flow curve empiricism[11,12] along with the parameter characterization of Rohlfing and Janzen,[13] we can obtain a modified Carreau-Yasuda equation:

$$\eta(\dot\gamma) = \frac{C_1 \overline{M_w}^{C_2}}{[1 + (C_1 C_3 \overline{M_w}^{C_2}\dot\gamma)^{C_4}]^{C_5/C_4}} \tag{1}$$

η is the steady-shear non-Newtonian viscosity, $\dot\gamma$ is the shear rate, $\overline{M_w}$ is the weight-average molecular weight, and C_1-C_5 are correlation parameters. The two constants C_1 and C_2 are equal to the associated values for the zero-shear viscosity relationship $\eta_0 = A\overline{M_w}^B$. For a large selection of linear low-density polyethylenes at 190 °C, Rohlfing and Janzen[13] found that $A = 5.8 \times 10^{-14}$ Pa s and $B = 3.41$.

They also gave approximate values for the remaining parameters: $C_3 = 2.50 \times 10^{-6}$ Pa^{-1}, $C_4 \sim 1$, and $C_5 = 0.82$. The value of C_4 is usually a positive number less than 2. The value of C_5 is fixed in Rohlfing and Janzen's work[13]—it comes from Graessley's theory for the flow curve of monodisperse melts.[14] We treat the first four parameters as adjustable and the fifth parameter as fixed.

2. Correlating the Flow Curve with the Entire MWD. Bersted's partition model[6,7] correlates the entire MWD and flow curve for linear polymers. Despite its simplicity, it is very successful. As a result, research efforts[15−22] typically focus on the intricacies of the so-called inverse problem, that is, to predict the MWD from the flow curve. Very few papers focus on converting the MWD to the flow curve —an example is Mavridis and Shroff.[10]

Bersted's partition model[6,7] relates the non-Newtonian shear viscosity $\eta(\dot\gamma)$ to a partitioned weight-average molecular weight $\overline{M_w^*}$ through two constants K_1 and K_2:

$$\eta(\dot\gamma) = K_1 \overline{M_w^*}^{K_2} \tag{2}$$

Bersted[6] computed the partitioned weight-average molecular weight using the MWD:

$$\overline{M_w^*} = \sum_{i=1}^{c-1} w_i M_i + M_c \sum_{i=c}^{N} w_i \tag{3}$$

The MWD contains N points of (M_i, w_i) data, where M_i is the molecular weight for point i and w_i is the corresponding weight fraction. Point c is some point in the distribution characterized by a critical molecular weight M_c (not to be confused with the critical molecular weight for the onset of entanglement), which is computed below:

$$M_c = K_3 \dot\gamma^{-K_4/K_2} \tag{4}$$

We can approximate the two constants K_1 and K_2 in eq 2 by the associated values for the zero-shear viscosity relationship $\eta_0 = A\overline{M_w}^B$. For a large selection of linear low-density polyethylenes at 190 °C, Rohlfing and Janzen[13] found that $A = 5.8 \times 10^{-14}$ Pa s and $B = 3.41$.

The value of K_3 is theoretically equal to the power law constant m (as in the fit to the power law region $\eta(\dot\gamma) = m\dot\gamma^{n-1}$) divided by K_1. Bersted and Slee[7] used $K_3 = 5.4 \times 10^5$ g/mol·s$^{K_4/K_2}$ for HDPE at 190 °C. The value

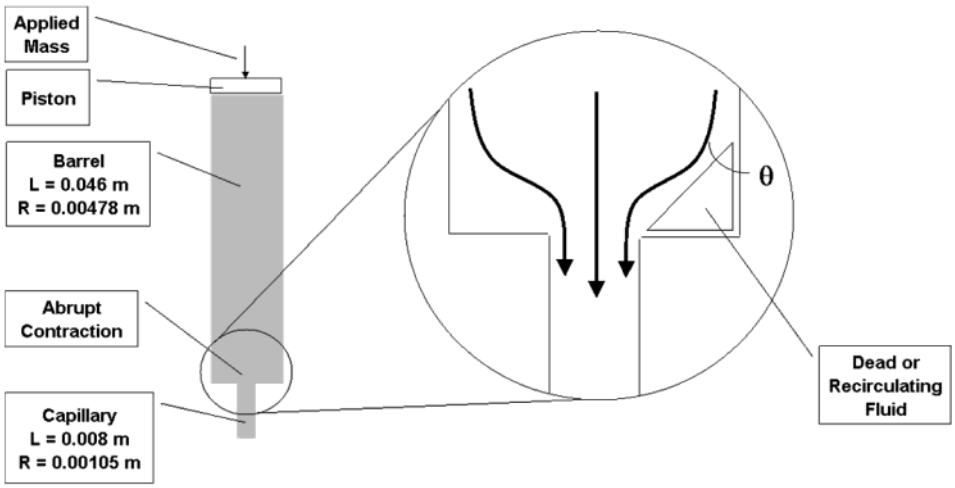

Figure 2. Melt-flow plastometer for melt-index determination. The polymer melt flows through the barrel, entrance region (or contraction), and capillary. The blow-up depicts the entrance region, where funneling flow takes place.

of K_4 is theoretically equal to the power law constant n. Graessley's theory for the flow curve of monodisperse melts[14] points to a value of 0.8, but Bersted and Slee[7] found better success in modeling HDPE by setting this parameter to 1.

Correlating the MI with the Weight-Average Molecular Weight. The MI is usually correlated with the MWD using an empirical model, such as the one proposed by Bremner and Rudin:[8]

$$1/\mathrm{MI} = G\overline{M_w}^{x} \tag{5}$$

This simple model and its variations are extremely successful for linear polymers. Thus, it is the standard for predicting the MI of polyolefins in polymer process simulations. When we regress the linear low-density polyethylene (LLDPE) data in the Bremner and Rudin paper,[8] we find that G ranges from 2×10^{-20} to 1×10^{-24} (units of 10 min g^{-1-x} mol^x) and x ranges from 3.9 to 4.6.

Predicting the MI from the Flow Curve. Predicting the MI using only the flow curve calls for a fundamental model. Fundamental models for the MI employ a parameter-free fluid mechanics description of the melt indexer, which is a rheometer barrel terminated with a short capillary (Figure 2).

Melt-indexer models essentially translate rheological information into a corresponding MI. Two classes are (1) finite-element models and (2) approximations. We will disregard completely the prediction of MI using finite-element methods—these are prohibitive because (1) the computation time is too high and (2) the data requirements, which include viscoelastic material functions and a suitable constitutive equation, are overwhelming to modelers of polymer manufacturing processes.

Models for the melt indexers are only approximate because of the entrance pressure drop estimation (see Figure 2). A precise equation for the entrance pressure drop might contain contributions from the shear viscosity and the unsteady elongational viscosity. To our knowledge, Rohlfing and Janzen[9] presented the only approximate model for the melt indexer. However, they have not validated the predictive power of their model with experimental data.

Rohlfing and Janzen[9] considered the total pressure drop in the melt indexer as a sum of the pressure drops in the barrel, entrance region, and the capillary. The sum of the pressure drops is equal to the applied pressure:

$$P_b + P_e + P_c = Mg/\pi R_p^{\,2} \tag{6}$$

P_b (Pa) is the barrel pressure drop, P_e (Pa) is the entrance pressure drop, and P_c (Pa) is the capillary pressure drop. The applied mass is M (kg), the gravity constant is g (m/s^2), and the radius of the piston is R_p (m).

Rohlfing and Janzen[9] computed the volumetric flow rate Q (m^3/s) for fully developed, pressure-driven flow in both the barrel (i = b) and cylinder (i = c) below:

$$Q = \frac{\pi R_i^{\,3}\dot{\gamma}_{R_i}}{3} - \frac{\pi}{3}\left(\frac{2L_i}{P_i}\right)^3 \int_0^{\dot{\gamma}_{R_i}} (\eta(\dot{\gamma})\dot{\gamma})^3 \, \mathrm{d}\dot{\gamma} \tag{7}$$

$$\dot{\gamma}_{R_i}\eta(\dot{\gamma}_{R_i}) = P_i R_i/2L_i \tag{8}$$

R_i is the radius of cylinder I (m), $\dot{\gamma}_{R_i}$ is the shear rate at the wall of cylinder I (1/s), L_i is the length of cylinder i (m), and P_i is the pressure drop in cylinder i (Pa). One may argue that fully developed flow does not exist in the relatively short capillary; Rohlfing and Janzen[9] showed that the entrance length is most likely negligible in computing the MI.

Rohlfing and Janzen[9] estimated the entrance pressure drop using Cogswell's equation:[23]

$$P_e = \frac{4\sqrt{2}\dot{\gamma}_a}{3(n'+1)}\sqrt{\eta(\dot{\gamma}_a)\eta_e(\dot{\epsilon})}\left(\frac{4n'}{3n'+1}\right)^{(1+n'/2)} \tag{9}$$

$\dot{\gamma}_a$ is the apparent shear rate (1/s), η_e is the elongational viscosity (Pa s), $\dot{\epsilon}$ is the elongation rate (1/s), and n' is the flow curve slope index.

The apparent shear rate in the capillary is related to the true shear rate at the capillary wall through the following equation:

$$\dot{\gamma}_a = \frac{4}{3 + 1/n'}\,\dot{\gamma}_{Rc} \tag{10}$$

Table 1. Physical Constants Used in Melt-Index Computations

physical constant	value
piston radius (R_p, m)	0.004737
barrel radius (R_b, m)	0.004775
barrel length (L_b, m)	0.046
capillary radius (R_c, m)	0.00105
capillary length (L_c, m)	0.008
applied pressure (P, Pa, for a 2.16-kg mass)	300,265.1
melt density at 463 K (190 °C, kg/m^3)	758.727

Since we do not have the elongational viscosity as a function of elongation rate, we estimate it using a modified Trouton's rule, in which the Trouton ratio[24] is set to 3:

$$\eta_e(\dot{\epsilon}) \sim 3\eta(\dot{\epsilon}) \tag{11}$$

Rohlfing and Janzen[9] gave the approximate elongation rate:

$$\dot{\epsilon} = \frac{4\eta(\dot{\gamma}_a)\dot{\gamma}_a}{3(n'+1)P_e}\left[\frac{4n'}{3n'+1}\right]^{n'+1} \tag{12}$$

They computed the flow curve slope index n' below:

$$n' = \frac{\mathrm{d}\log\eta(\dot{\gamma}_a)}{\mathrm{d}\log\dot{\gamma}_a} + 1 \tag{13}$$

We solve the nonlinear equation set consisting of seven equations, namely, eq 6−8 for both barrel and capillary, eqs 9 and 10, for seven variables: the shear rate at the barrel wall ($\dot{\gamma}_{R_b}$, 1/s), the shear rate at the capillary wall ($\dot{\gamma}_{R_c}$, 1/s), the apparent shear rate in the capillary ($\dot{\gamma}_a$, 1/s), the barrel pressure drop (P_b, Pa), the capillary pressure drop (P_c, Pa), the entrance pressure drop (P_e, Pa), and the volumetric flow rate (Q, m^3/s).

After obtaining the volumetric flow rate, we make a change of units to obtain the melt index using the melt density ρ:

$$\text{MI, g/10 min} = (Q, \text{m}^3/\text{s})(\rho, \text{kg/m}^3)(1000\ \text{g/1 kg})(600\ \text{s/10 min}) \tag{14}$$

We estimate the density of a polyethylene melt at 190 °C using the correlation in Rudin et al.[25]

$$\frac{1}{\rho, \text{g/cm}^3} = 1.282 + 9.0\times10^{-4}(T - 150\ °\text{C}) \tag{15}$$

Table 1 summarizes the physical constants used in computing the MI.

For a Newtonian fluid with viscosity μ, an analytical solution of Rohlfing and Janzen's equations is possible:

$$Q = \frac{mg}{8R_p^2\mu}\left[\frac{L_b}{R_b^4} + \frac{L_c}{R_c^4}\left(\frac{\sqrt{6}}{3}\frac{R_c}{L_c} + 1\right)\right]^{-1} \tag{16}$$

For the constants in Table 1, this reduces to $Q \sim 1.60\times10^{-5}/\mu$, where Q is in m^3/s and μ is in Pa s. In terms of the melt index, eq 16 reduces to MI $\sim 7.28\times10^3/\mu$.

Materials and Methods

Materials. We obtain three commercial LLDPE's produced using a single-site catalyst technology. We measure their MWDs and their flow curves—the MIs are those reported by the manufacturer—1.0, 3.5, and 4.5 g/10 min for LLDPEs 1, 2, and 3, respectively.

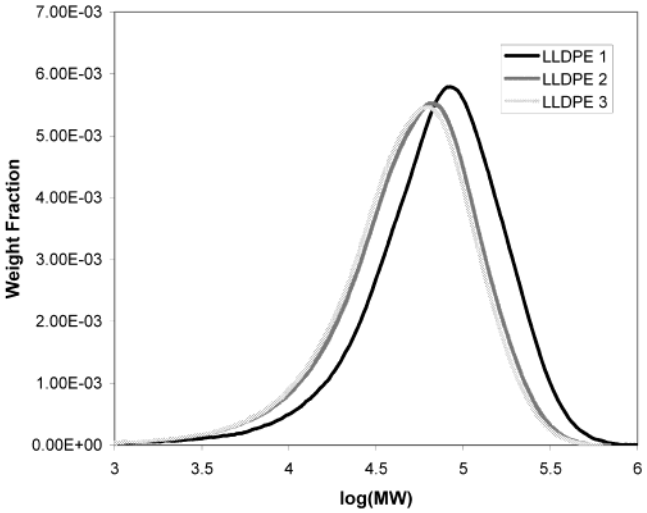

Figure 3. Molecular weight distributions for the three LLDPEs used in this study.

Table 2. Molecular Weight Averages for the Three LLDPEs Used in This Study

polymer sample	MWN (g/mol)	MWW (g/mol)	MWZ (g/mol)	MI (g/10 min)
1	39 800	91 000	154 000	1.0
2	30 000	67 000	111 000	3.5
3	28 700	62 500	105 000	4.5

We complete the molecular weight analyses using a Waters model 150C GPC apparatus, utilizing 1,2,4-trichlorobenzene solvent, operating at a temperature of 145 °C. To minimize degradation during sample preparation and analysis, we load the solvent with a small amount (nominally 0.1% w/w) of a thermal stabilizer and primary antioxidant, such as Irganox 1010. We calibrate the GPC column set using narrow-distribution polystyrene standards. We use an internally mounted differential refractive index detector for all samples. Table 2 lists the number , weight , and Z averages for the MWD and MIs and Figure 3 shows the MWDs.

We measure the flow curves at 190 °C using a standard force-driven capillary rheometer with a pressure transducer sensor at the base of the barrel. The die length/diameter ratio is 24, with a die diameter of 0.018 in. Once loaded, the sample is held in the barrel for a period of 5−6 min to ensure proper heating. Figure 4 shows the flow curves for the three polymers.

Unfortunately, the Newtonian plateau is not well resolved for LLDPE 1—however, it is partially resolved for LLDPEs 2 and 3.

Methods. We characterize the MWD/rheology data using relationships given in the Introduction. In particular, we ascertain correlative/predictive relationships between the MWD, flow curve, and MI: (a) correlate the flow curve and MI with the MWD; (b) correlate the flow curve with MWD and predict the MI; (c) correlate the MI with MWD and predict the flow curve.

We do so using the methods given below. We perform our numerical analysis using IMSL Version 2.0 FORTRAN subroutines (http://www.vni.com/products/imsl/). We use RNLIN to perform nonlinear regression, NEQNF to solve a nonlinear system of equations, and QDAGS to perform numerical integration. We use RCOVB and TIN to estimate the 95% confidence intervals when performing nonlinear regression.

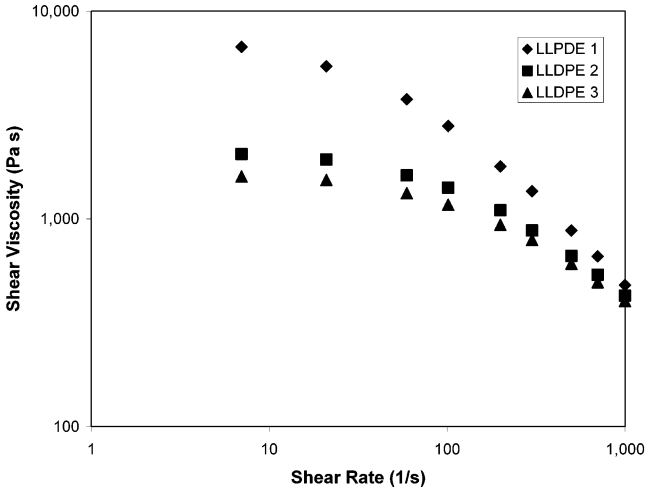

Figure 4. Flow curves for the three LLDPEs used in this study.

1. Correlating the Flow Curve and MI with the MWD. In this case, we generate independently the relationship between the MWD and flow curve and the relationship between the MWD and MI (see Figure 1a).

We use the modified CY or Bersted model (under Correlating the Flow Curve with the MWL) to correlate the MWD and flow curve. We determine the two, four-parameter sets C_1-C_4, eq 1, and K_1-K_4, eqs 2 and 4, using nonlinear regression. We again use nonlinear regression to determine the Bremner/Rudin parameters G and x, eq 5. This correlates the weight-average molecular weight and the MI.

2. Correlating the Flow Curve with the MWD and Predicting the MI. We correlate the MWD and the flow curve and then directly use these flow curve correlations to predict the MI (see Figure 1b).

Using the CY or Bersted model correlation obtained in subsection 1, we predict the MI using Rohlfing and Janzen's MI model[9] described (under Predicting the MI from the Flow Curve). This model is a nonlinear system of equations. We use the Newtonian solution as the initial guess and numerical integration to evaluate eq 7.

3. Correlating the MI with the MWD and Predicting the Flow Curve. In this last option, we generate a correlation between the MWD and the MI. In doing so, we generate predictions for the flow curve (see Figure 1c).

We combine the CY or Bersted's model with Rohlfing and Janzen's model to predict the MI using the MWD. We use nonlinear regression to obtain the CY or and Bersted parameters that generate the best MI predictions.

Results and Discussion

Correlating the Flow Curve and MI with the MWD. We regress the modified Carreau-Yasuda parameters that produce the best MWD/flow curve correlation. Figure 5 shows the CY model flow curves compared with experimental data.

The average absolute error over all viscosity points is 3%. Table 3 shows the parameter estimates.

All of the values seem relatively well determined, except for the value of C_1. This is because of the lack of data in the Newtonian region.

Figure 6 shows similar regression results for the Bersted model.

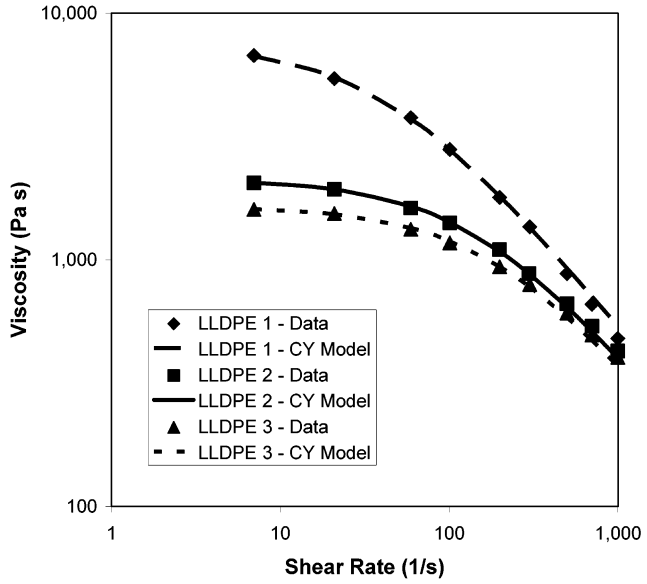

Figure 5. Correlation of the weight-average molecular weights and the flow curves using the modified Carreau-Yasuda model.

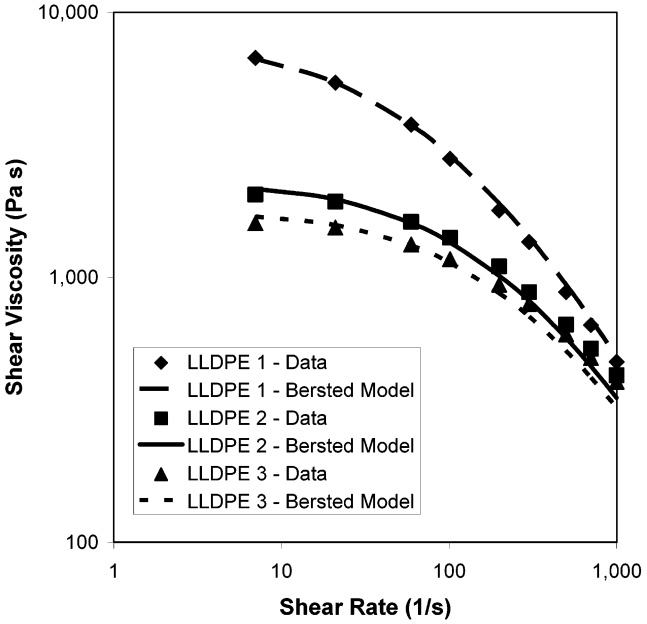

Figure 6. Correlation of the MWDs and the flow curves using Bersted's partition model.[6,7]

Table 3. Modified Carreau-Yasuda Model Parameters Gained through Correlating the Weight-Average Molecular Weights and the Flow Curves for the Three LLDPEs

parameter	value	95% confidence interval (%)
C_1	7.84×10^{-17}	±63.2
C_2	4.03	±1.39
C_3	3.23×10^{-6}	±4.15
C_4	1.05	±9.14

The Bersted correlation also appears quite good—The average correlation error is 7%. Table 4 shows the corresponding Bersted parameters.

The values for the parameters K_2-K_4 are well determined—their confidence intervals are small. However, the parameter K_1 is not well determined. This is because of the lack of data in the Newtonian region, as in the case for the determination of the CY model parameters.

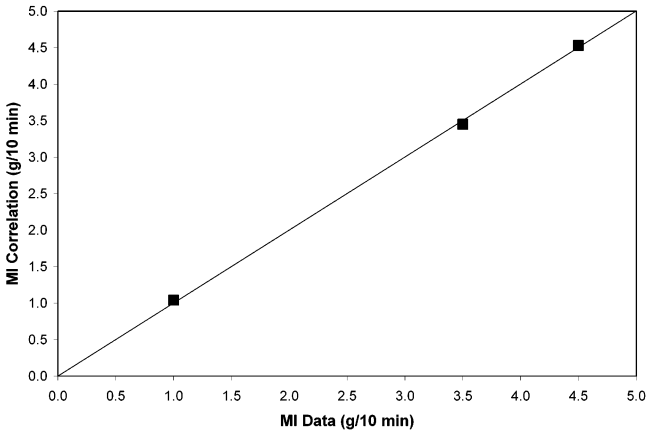

Figure 7. Correlation of the weight-average molecular weight and the melt index using Bremner and Rudin's model: MI prediction vs experimental data.

Table 4. Bersted Model Parameters Gained through Correlating the MWDs and the Flow Curves for the Three LLDPEs

parameter	value	95% confidence interval (%)
K_1	4.72×10^{-16}	±140
K_2	5.01×10^{5}	±13.3
K_3	1.26	±5.74
K_4	3.87	±3.22

Last, we characterize the parameters of the Bremner and Rudin's empirical MI model,[8] eq 5. Figure 7 compares the resulting MI predictions with experimental data.

The fit is quite good—the average error is 2%, which is below the experimental repeatability of the MI measurement, ~7%.[1] The correlation is below:

$$\frac{1}{\text{MI, g/10 min}} = 3.63 \times 10^{-20}(\overline{M_w}, \text{g/mol})^{3.92} \quad (17)$$

The 95% confidence interval for the first parameter is ±2456% and that for the second parameter is ±57%. These high values result from the low number of data points compared to the number of parameters being regressed.

Correlating the Flow Curve with the MWD and Predicting MI. This case differs from the previous one because we suppose that we lack MI data. Therefore, we cannot create a Bremner/Rudin correlation.[8]

Instead, we take the CY or Bersted model prediction for flow curves (parameters in Table 3 and Table 4) and compute the MI using the Rohlfing–Janzen model for the melt indexer.[9] Figure 8 shows the MI predictions compared with experimental data.

The parameter-free Rohlfing–Janzen model[9] works well for converting the flow curve into the MI—the average prediction errors are −0.5 and −3% for the CY and Bersted models, respectively. These errors are well below the experimental repeatability of the data themselves. The shear rate at the capillary wall, $\dot{\gamma}_{R_c}$ (eq 8), is estimated as 2.4, 8.2, and 10.0 s^{-1} for LLDPEs 1–3, respectively.

Since $\dot{\gamma}_{R_c}$ is low and the MI computation considers viscosities in the range of $0-\dot{\gamma}_{R_c}$ (see the integral in eq 7), we have essentially relied on the modified Carreau-Yasuda or Bersted[6] model to extrapolate our viscosity data to the Newtonian plateau. Despite the large statistical variability of C_1 and K_1 in our case, the good

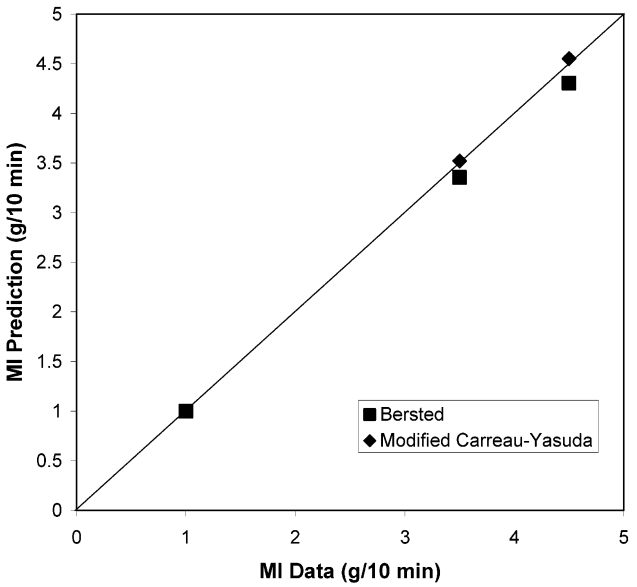

Figure 8. MI prediction generated from the Rohlfing–Janzen model with flow curves generated by the Bersted and modified Carreau-Yasuda model and the parameters of Table 3 and Table 4: prediction vs experimental data.

MI predictions suggest that the CY and Bersted[6] models were successful in resolving the Newtonian plateaus.

Conservatively though, we recommend that if our goal is to predict the MI from the flow curve, then we should collect flow curve data that span the range of the shear rates experienced in the melt indexer ($\sim 0-\dot{\gamma}_{R_c}$). In addition, the MI prediction should always be validated to ensure that the entrance pressure drop prediction, eq 9, is approximately correct. This computation is the source of the empiricism in the Rohlfing–Janzen model and could fail if the polymers display nonideal elongational behavior such as strain hardening. Rohlfing and Janzen[9] corrected failures in the entrance pressure drop prediction by increasing the Trouton ratio from 3 up to 10. We find that 3 is adequate for our particular samples.

Correlating the MI with the MWD and Predicting the Flow Curve. In our final analysis, we consider the case in which we only have MWD/MI data and we want to predict the flow curves. This problem is drastically different from that of correlating the MWD/flow curve—it is much more difficult statistically because the number of data points we are regressing is much smaller. In correlating the MWD/flow curves, we regress four parameters using 27 flow curve data points. In this case, we can regress up to four parameters using three MI data points.

Because we only have three MI data points, we choose to consider only two subcases instead of attempting to regress all four CY or Bersted parameters: (a) We consider the viscosity to be Newtonian and compute this viscosity from the melt index (MI $\sim 7.28 \times 10^3/\mu$). We then regress these viscosities to determine the values of the two parameters in $\eta_0 = A\overline{M_w}^B$. $A = C_1$ and $B = C_2$ in the Newtonian case of the modified CY model, with $C_3 = 0$ and C_4 set to any value (we use 1). For the Newtonian case of the Bersted model, $A = K_1$ and $B = K_2$, with K_3 set to a high value such as 1×10^{20} and K_4 set to any value (we use 1). (b) We consider the viscosity to be non-Newtonian, and attempt to regress C_3 and K_3 in addition to the first two parameters. We leave C_4 and K_4 set to 1.

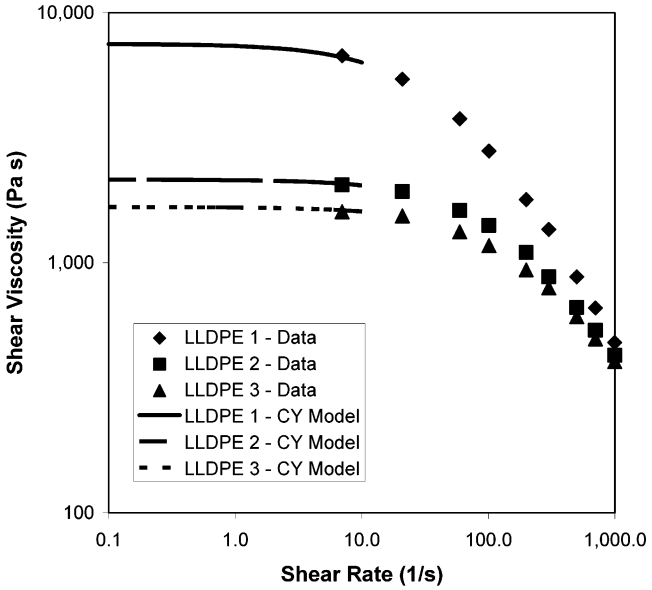

Figure 9. Equivalent Newtonian viscosity prediction compared with the flow curve data.

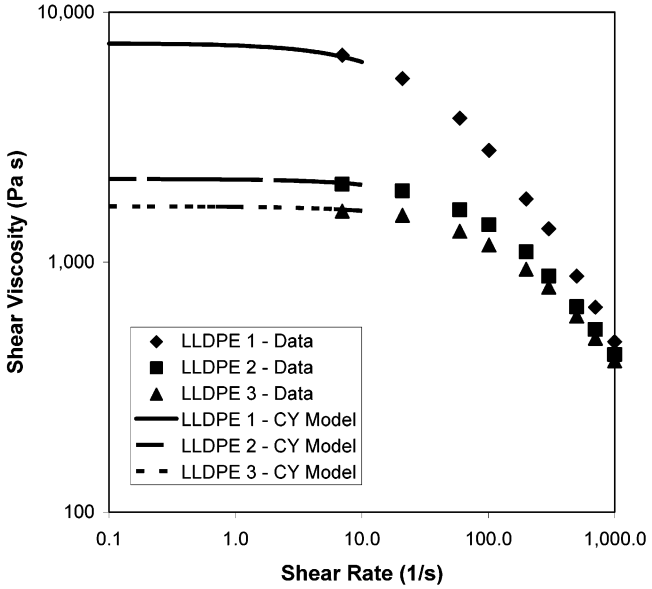

Figure 10. Non-Newtonian viscosity prediction using MWW/MI data and the combined modified Carreau-Yasuda/Rohlfing−Janzen model (parameters C_1, C_2, and C_3 regressed and C_4 fixed to 1).

Figure 9 shows the equivalent Newtonian viscosity predictions compared with the flow curves.

The predicted MIs are 1.02, 3.50, and 4.50 g/10 min for LLDPEs 1, 2, and 3, respectively. The parameters for Newtonian viscosity model are below:

$$\eta_0, \text{ Pa s} = 6.25 \times 10^{-17}(\overline{M_w}, \text{ g/mol})^{4.05} \qquad (18)$$

The 95% confidence interval for the A value is ±700% and for B it is ±15.1%. Again, there is a considerable amount of noise in the A determination—we attribute this to the fact that we are regressing two parameters using only three MI predictions.

We now attempt to correlate the third parameter—C_3 in the case of the modified Carreau-Yasuda model. Figure 10 shows the flow curve predictions.

The regressed parameters are $C_1 = 1.08 \times 10^{-16}$ Pa s, $C_2 = 4.00$, and $C_3 = 3.11 \times 10^{-6}$ Pa^{-1}.

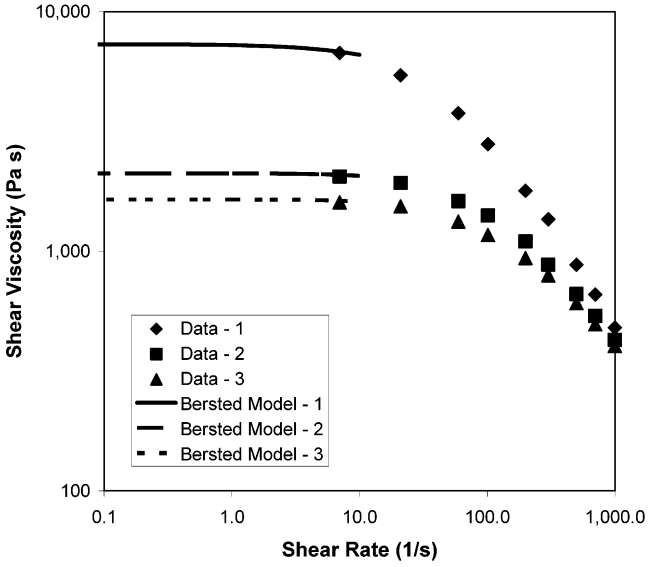

Figure 11. Non-Newtonian viscosity prediction using MWD/MI data and the combined Bersted/Rohlfing−Janzen model (parameters K_1, K_2, and K_3 regressed and K_4 fixed to 1).

Similarly, for the Bersted model, when we attempt to correlate K_3 in addition to the two parameters K_1 and K_2, we obtain the low-shear flow curve predictions in Figure 11.

The regressed parameters are $K_1 = 1.60 \times 10^{-16}$, $K_2 = 3.97$, and $K_3 = 4.04 \times 10^5$, and the MIs are the same as in the Newtonian case.

We could not compute the confidence intervals in both cases because the number of parameters is equal to the number of data points. However, these values must be quite large, indicating that the solution is not unique (i.e., multiple predicted flow curves give equally good MI predictions). In fact, the solution depends heavily on the initial guesses for the parameters. We may be able to overcome this problem by increasing the number of MWD/MI data points so that the number of data points is much larger than the number of parameters that we are attempting to determine. We will also have to include samples whose melt-index measurements cover the power law region of their flow curve.

This alerts us to a considerable limitation of predicting the flow curve from the MI and MWD. Even if the flow curve estimation procedure is perfect, we cannot expect this method to predict regions of the flow curve that lie outside the shear rate range of the melt indexer. What we mean is that if none of the shear-thinning region is involved in the MI computation (as in our case), then we cannot confidently predict the shear-thinning viscosity. However, if part of the power law region of the flow curve is experienced in the MI measurement, then there is hope of predicting the entire flow curve given enough MWD/MI data points. In our case, the MI measurements only include the Newtonian region—therefore, we are only able to estimate the Newtonian viscosity.

Conclusions and Recommendations

We have characterized the relationships among the MWD, the flow curve, and the MI for three LLDPEs produced using the same single-site catalyst and process technology. We relate (1) the flow curve and MWD using either a modified Carreau-Yasuda or Bersted partition model, (2) the MI and MWD using Bremner and Rudin's

model, and (3) the flow curve and the MI using Rohlfing and Janzen's model.

Both the modified Carreau-Yasuda and Bersted models successfully correlate the MWD and flow curve for the three LLDPEs, producing four parameters. Statistical uncertainty is present in the zero-shear viscosity preexponential factor, presumably due to a lack of data in the Newtonian region of the flow curves. Similarly, Bremner and Rudin's model easily correlates the weight-average molecular weight and MI data for these three polymers.

We compute the MIs accurately using Rohlfing and Janzen's fluid mechanics model and flow curves predicted by either the modified Carreau-Yasuda or Bersted model. However, when attempting to predict the flow curve from MWD/MI data only, we are only able to resolve the Newtonian region of the flow curves because the capillary wall shear rates are low in the melt-index measurement (<10 1/s).

In light of these observations, we recommend the following guidelines for polymer process modelers: (a) When developing the MWD/flow curve relationship using either the modified Carreau-Yasuda or Bersted's model, the flow curves should contain data points in the shear rate range and temperature of interest. If we use flow curves to predict only the MI, then this shear rate range extends from 0 to the wall shear rate of the capillary. If we want to do processing computations though, the upper limit of the shear rate range could be many orders of magnitude higher than that experienced in the melt indexer. (b) When computing the MI from the flow curve, the MI prediction should always be compared with the experimental values. This will protect us from extrapolation errors made by the modified Carreau-Yasuda or Bersted model or errors generated by Cogswell's entrance pressure-drop approximation.

(c) When estimating the flow curve from MWD/MI data alone, many data points are needed. In addition, a realistic target is to estimate only that portion of the flow curve that is experienced in the melt indexer. Once again, predictions should always be compared with experimental measurements to guard us from errors generated by Cogswell's approximation or the possibility that multiple, different flow curves satisfy the MWD/MI relationship equally well.

Acknowledgments

We thank Alliant Techsystems, Aspen Technology (particularly Dustin MacNeil, Director of Worldwide University Programs, and Larry Evans, Board Chairman), China Petroleum and Chemical Corp. (particularly Xianghong Cao, Senior Vice President), and Honeywell Specialty Materials and the Honeywell International Foundation for supporting the educational programs in computer-aided design and process systems engineering at Virginia Tech.

Nomenclature

A = Newtonian viscosity preexponential factor (Pa s g^{-B} mol^{B})
B = Newtonian viscosity exponent (unitless)
C_i = modified Carreau-Yasuda model parameters ($i = 1-4$) (varies)
G = Bremner/Rudin constant (10 min g^{-1-x} mol^{x})
g = gravitional acceleration constant (m/s^2)
K_i = Bersted model parameters ($i = 1-4$) (varies)
L_i = length of i (barrel, capillary) (m)
M = melt-indexer applied mass (kg)
m = power law constant (Pa s^n)
M_c = critical molecular weight in Bersted model (g/mol)
M_i = molecular weight i in molecular weight distribution (g/mol)
$\underline{M_w}$ = weight-average molecular weight (g/mol)
M_w^* = Bersted model partitioned weight-average molecular weight (g/mol)
MI = melt index (g/10 min)
n = power law exponent (unitless)
n' = instantaneous power law exponent (unitless)
P_i = pressure drop in region i (barrel, entrance, capillary) (Pa)
Q = volumetric flow rate (m^3/s)
R_i = radius of i (barrel, capillary, piston (m)
T = temperature (°C)
w_i = weight fraction of molecular weight i in molecular-weight distribution (unitless)
x = Bremner/Rudin exponent (unitless)
$\dot{\epsilon}$ = elongation rate (s^{-1})
$\dot{\gamma}$ = shear rate (s^{-1})
$\dot{\gamma}_a$ = apparent shear rate in capillary (s^{-1})
$\dot{\gamma}_{R_i}$ = wall-shear rate in i (barrel, capillary) (s^{-1})
μ = Newtonian viscosity (Pa s)
η = steady-shear non-Newtonian viscosity (flow curve) (Pa s)
η_0 = zero-shear viscosity (Pa s)
η_ϵ = steady elongational viscosity (Pa s)
ρ = melt density (kg/m^3)

Literature Cited

(1) ASTM Subcommittee D20.30. Standard Test Method for Flow Rates of Thermoplastics by Extrusion Plastometer. *ASTM Standard Method D 1238-00*, 2000.

(2) Baird, D. G.; Collias, D. I. *Polymer Processing: Principles and Design*; Wiley: New York, 1998; pp 16, 31, 207.

(3) Shenoy, A. V.; Saini, D. R. Melt Flow Index: More Than Just a Quality Control Rheological Parameter. Part I. *Adv. Polym. Technol.* **1986**, *6*, 1−58.

(4) Bokis, C. P.; Ramanathan, S.; Franjione, J.; Buchelli, A.; Call, M. L.; Brown, A. L. Physical Properties, Reactor Modeling, and Polymerization Kinetics in the Low-Density Polyethylene Tubular Reactor Process. *Ind. Eng. Chem. Res.* **2002**, *41*, 1017−1030.

(5) Khare, N. P.; Seavey, K. C.; Liu, Y. A.; Ramanathan, S.; Lingard, S.; Chen, C. C. Steady State and Dynamic Modeling of Commercial Slurry High-Density Polyethylene Processes. *Ind. Eng. Chem. Res.* **2002**, *41*, 5601−5618.

(6) Bersted, B. H. An Empirical Model Relating the Molecular Weight Distribution of High-Density Polyethylene to the Shear Dependence of the Steady-Shear Melt Viscosity. *J. Appl. Polym. Sci.* **1975**, *19*, 2167−2177.

(7) Bersted, B. H.; Slee, J. D. A Relationship Between Steady-State Shear Melt Viscosity and Molecular Weight Distribution in Polystyrene. *J. Appl. Polym. Sci.* **1977**, *21*, 2631−2644.

(8) Bremner, T.; A. Rudin, Melt Flow Index Values and Molecular Weight Distributions of Commercial Thermoplastics. *J. Appl. Polym. Sci.* **1990**, *41*, 1617−1627.

(9) Rohlfing, D. C.; Janzen, J. What is Happening in the Melt-Flow Plastometer: The Role of Elongational Viscosity. *Ann. Tech. Conf.−Soc. Plast. Eng.* **1997**, 1010−1014.

(10) Mavridis, H.; Shroff, H. Appraisal of a Molecular Weight Distribution-to-Rheology Conversion Scheme for Linear Polyethylenes. *J. Appl. Polym. Sci.* **1993**, *49*, 299−318.

(11) Elbirli, B.; Shaw, M. T. Time Constants from Shear Viscosity Data. *J. Rheol.* **1978**, *22*, 561.

(12) Yasuda, K.; Armstrong, R. C.; Cohen, R. E. Shear Flow Properties of Concentrated Solutions of Linear and Star Branched Polystyrenes. *Rheol. Acta* **1981**, *20*, 163.

(13) Rohlfing, D. C.; Janzen, J. Melt Rheological Characteristics of Metallocene Catalyzed Polyethylenes. In *Metallocene-based Polyolefins*; Scheirs, J., Kaminsky, W., Eds.; John Wiley and Sons: New York, 2000; pp 419−434.

(14) Graessley, W. W. Viscosity of Entangling Polydisperse Polymers. *J. Chem. Phys.* **1967**, *47*, 1942−1953.

(15) Tuminello, W. H. Relating Rheology to Molecular Weight Properties of Polymers. In *Encyclopedia of Fluid Mechanics, Volume 9: Polymer Flow Engineering*; Cheremisinoff, N. P., Ed.; Gulf Publishing Co.: Houston, 1990; pp 209−242.

(16) Tuminello, W. H. Molecular Weight and Molecular Weight Distribution from Dynamic Measurements of Polymer Melts. *Polym. Eng. Sci.* **1986**, *26*, 1339−1347.

(17) Tuminello, W. H. Determination of Molecular Weight Distribution (MWD) from Melt Rheology: A Review. *Ann. Tech. Conf.−Soc. Plast. Eng.* **1987**, 990−996.

(18) Tuminello, W. H. Determining Molecular Weight Distributions from Viscosity vs Shear Rate Flow Curves. *Polym. Eng. Sci.* **1991**, *31*, 1496−1507.

(19) Malkin, A. Y.; Teishev, A. E. Flow Curve-Molecular Weight Distribution: Is the Solution to the Inverse Problem Possible? *Polym. Eng. Sci.* **1991**, *31*, 1590−1596.

(20) Wood-Adams, P. M.; Dealy, J. M. Use of Rheological Measurements to Estimate the Molecular Weight Distribution of Linear Polyethylene. *J. Rheol.* **1996**, *40*, 761−778.

(21) Liu, Y.; Shaw, M. T.; Tuminello, W. H. Obtaining Molecular Weight Distribution Information from the Viscosity Data of Linear Polyethylene Melts. *J. Rheol.* **1998**, *42*, 453−476.

(22) Maier, D.; Eckstein, A.; Friedrich, C.; Honerkamp, J. Evaluation of Models Combining Rheological Data with the Molecular Weight Distribution. *J. Rheol.* **1998**, *42*, 1153−1173.

(23) Cogswell, F. N. Converging Flow of Polymer Melts in Extrusion Dies. *Polym. Eng. Sci.* **1972**, *12* (1), 64−73.

(24) Bird, R. B.; Armstrong, R. C.; Hassager, O. *Dynamics of Polymeric Liquids*, 2nd Ed.; Wiley: New York, 1987; Vol. 1, p 39.

(25) Rudin, A.; Chee, K. K.; Shaw, J. H. Specific Volume and Viscosity of Polyolefin Melts. *J. Polym. Sci., Part C* **1970**, *30*, 415−427.

Received for review December 12, 2002
Revised manuscript received August 12, 2003
Accepted August 12, 2003

IE021003I